ACKNOWLEDGMENTS

We would like to acknowledge the indispensable assistance in this experiment of W. Beck, H. Kuhn, L. Griffith, and C. Symons of CERN, and of E. Coleman, B. Loo, and S. Powell of The University of Michigan. A major part of the analysis was carried out at The University of Michigan including film measurement and digital calculation, and was supported by the U. S. Office of Naval Research Contract No. Nonr 1224(23). Film measurements at M.I.T. were supported by the U. S. Atomic Energy Commission. Valuable assistance in film prescanning was carried out at the University of Bologna under the direction of G. Giacomelli. We have benefited significantly from discussions on the theoretical interpretations of these data with G. Chew, R. Deck, S. Drell, C. Lovelace, and B. Svensson. Finally, it is a pleasure to express our gratitude to CERN for its hospitality during the course of this experiment and the subsequent analysis.

PHYSICAL REVIEW VOLUME 166, NUMBER 5 25 FEBRUARY 1968

Four- and Five-Body Final States from 3-GeV/c π^-p Interactions*

A. W. KEY, J. D. PRENTICE, N. R. STEENBERG, E. WEST, AND T. S. YOON
University of Toronto, Toronto, Canada

AND

W. A. COOPER, W. MANNER, AND L. VOYVODIC
Argonne National Laboratory, Argonne, Illinois

AND

W. D. WALKER
University of Wisconsin, Madison, Wisconsin

(Received 25 August 1967)

Approximately 3600 four-prong events produced by π^-p interactions at 2.96 GeV/c have been analyzed. The $p\pi^+\pi^-\pi^-$ channel shows production of $N^{*++}(1238)$ [(41±4)%], ρ^0 [(40±5)%], and A_2^- [(7±2)%]. Some evidence for associated $N^{*0}\rho^0$ production is also observed. The one-pion-exchange mode with form factor is shown to give an adequate description of the $N^{*0}\rho^0$ events. The $N^{*++}\pi^-\pi^-$ events are analyzed within the framework of this model, and the $I=2$ $\pi\pi$ scattering cross section up to $m(\pi\pi)\simeq 1$ GeV/c^2 is calculated. A value for the $I=2$ $\pi\pi$ s-wave scattering length of $|a_2^0|=0.19m_\pi^{-1}$ is obtained. In a determination of the spin and parity of the A_2 meson, the 2^+ assignment is favored throughout the fairly wide range of experimental uncertainties in the estimate of the background in the A_2 region. The $p\pi^+\pi^-\pi^-\pi^0$ channel is dominated by production of ω^0 [(26±2)%] and $N^{*++}(1238)$ [(30±6)%]. ρ^-, ρ^0, and $N^{*+}(1238)$ are produced much more weakly. Peripherality is much less pronounced than in the four-constraint fits. No B meson is observed in the present data. The observation of enhancements at 2080 and 2190 MeV/c^2 in the $p\pi^+\pi^-\pi^0$ spectrum has been reported previously. The $n\pi^+\pi^+\pi^-\pi^-$ channel shows strong $N^{*-}(1238)$ production [(50±10)%] and some weak ρ^0 production.

I. INTRODUCTION

THIS paper presents an analysis of four-prong events produced by π^- mesons of 2.96 GeV/c in hydrogen. The two-prong events have been reported previously.[1] The events have been classified as

$$\pi^-p \rightarrow p\pi^+\pi^-\pi^-, \quad 1608 \text{ events (1)}$$
$$\rightarrow p\pi^+\pi^-\pi^-\pi^0, \quad 1412 \text{ events (2)}$$
$$\rightarrow \pi^+\pi^+\pi^-\pi^-n. \quad 620 \text{ events (3)}$$

Resonance production is observed in all these final states, but, in particular, reaction (1) is used to study $\pi\pi$ scattering in the $I=2$ channel and the decay of the A_2 meson; reaction (2) has indicated the production of a new N^* of mass 2080 MeV/c^2; and reaction (3) shows some anomalies in the production of known isobars. These topics are discussed in this order in the sections that follow. Many similar experiments have been carried out for pions up to about 4 GeV/c. References 2 and 3 contain full bibliographies.

The events were taken from an exposure of 50 000 pictures in the 30-in. ANL-MURA hydrogen bubble chamber at the Argonne ZGS. Seventy millimeter film and a high field (32 kG) allowed accurate measurements to be made using conventional film plane and image

* Work supported in part by the U. S. Atomic Energy Commission and the National Research Council of Canada.

[1] D. R. Clear, T. F. Johnston, J. Pilcher, J. D. Prentice, N. R. Steenberg, E. West, T. S. Yoon, W. A. Cooper, W. Manner, L. Voyvodic, and W. D. Walker, Nuovo Cimento **49A**, 399 (1967).

[2] Suh Urk Chung, Ph.D. thesis, University of California Radiation Laboratory UCRL Report No. 16881, 1966 (unpublished).

[3] P. R. Klein, R. J. Sahni, A. Z. Kovacs, and G. W. Tautfest, Phys. Rev. **150**, 1123 (1966) Aachen-Berlin-Birmingham-Bonn-Hamburg-London (I.C.)-München Collaboration, Nuovo Cimento **31**, 485 (1964).

plane digitizers with on-line computers. Ionization discrimination was used in those events where kinematic fitting left an ambiguity. Processing was carried out in parallel at Toronto with an IBM 7094 and at Argonne with a CDC 3600 using local versions of the Harwell geometry program and CERN GRIND and Berkeley SUMX. All film was scanned twice and remeasured where necessary. The absolute values of the cross sections quoted in this paper have been obtained by normalizing the cross section for reaction (1) to 1.80 mb.[4]

II. $p\pi^+\pi^-\pi^-$ CHANNEL

Effective-mass distributions for all possible particle combinations are shown in Fig. 1. $N^{*++}(1238)$ and ρ^0 productions dominate this channel. Breit-Wigner (BW) fits to these resonances are indicated by solid lines in Figs. 1(a) and 1(c). In the other diagrams, the phase-space distributions normalized to all events are indicated by solid lines. The deviations from phase space in the $\pi^-\pi^-$, $p\pi^+\pi^-$, and $p\pi^-\pi^-$ distributions are due to the reflection of the $N^{*++}(1238)$ production. A_2^- production is also observed [Fig. 1(g)].

The distribution of the production angle relative to the incident π^-, in the center-of-mass (c.m.) system for each of the final state particles, is presented in Fig. 2. The strong backward peak in the angular distribution of the proton is largely due to the peripheral production and subsequent decay of the $N^{*++}(1238)$. The peripheral production and subsequent decay of the $N^{*++}(1238)$. The peripheral production of ρ^0 and N^{*0} would also contribute to this peak and to the forward peak in the π^- angular distribution.

Section IIA describes the N^{*++} production channel and the analysis of this in terms of $\pi\pi$ scattering in the $I=2$ state. Section IIB describes ρ^0 and N^{*0} production. Section IIC presents a spin-parity analysis of the A_2 meson.

A. $N^{*++}(1238)$ Production and $\pi\pi$ Scattering

A BW fit[5] to the $p\pi^+$ effective mass distribution gave the following results:

Percentage N^{*++}	$(41\pm4)\%$
Central mass	1208 ± 4 MeV/c^2
Width	101 ± 12 MeV/c^2.

The production mechanism of N^{*++} in this channel has been discussed extensively in the past[2,3,6] and it is generally accepted that one-pion exchange (OPE) dominates. Additional evidence to support this view is presented here.

The peripheral nature of N^{*++} production is demonstrated in Fig. 3(a), where the 4-momentum transfer squared (Δ^2) to the $p\pi^+$ system is plotted for those events in the N^{*++} isobar region ($1.16<m(p\pi^+)<1.28$ GeV/c^2), and in Fig. 3(b), where the $m(p\pi^+)$ distribution for those events with $\Delta^2(p\pi^+)<0.8$ (GeV/c)^2 is plotted. Figure 3(c) gives the Treiman-Yang angular distributions for those N^{*++} events with $\Delta^2<0.8$ (GeV/c)^2. The peripheral nature of this production process is assumed to be a result of a OPE mechanism. The Feynman diagram for this process is shown in Fig. 4.

Theoretical treatments of this process ($\pi^-p\rightarrow N^{*++}\pi^-\pi^-$) have been given by various authors.[7,8] Following Ferrari and Selleri, the cross section is given by[9]

$$d^3\sigma/d\Delta^2dW^2dV^2=(1/16\pi^3)(1/m^2q_L^2)|F(\Delta^2)|^2Vq\sigma_{\pi\pi}\times(V,\Delta^2)Wp\sigma_{p\pi^+}(W,\Delta^2)/(\Delta^2+\mu^2)^2. \quad (2.1)$$

$F(\Delta^2)$ is the product of form factors coming from two vertices and a propagator. The $\pi\pi$ cross section off the mass shell, $\sigma_{\pi\pi}(V,\Delta^2)$, is given by

$$\sigma_{\pi\pi}(V,\Delta^2)=(q^{\rm off}/q)^{2l}\sigma_{\pi\pi}(V), \quad (2.2)$$

where $q^{\rm off}$ is the c.m. pion momentum in the initial state of the $\pi\pi$ system and l is the relative $\pi\pi$ orbital angular momentum. The off-shell $p\pi^+$ cross section $\sigma_{p\pi^+}(W,\Delta^2)$ in the N^* (1238) region is given by

$$\sigma_{p\pi^+}(W,\Delta^2)=(p^{\rm off}/p)^2[1+(\Delta^2+\mu^2)/4m^2]\times|G(\Delta^2)|^2\sigma_{p\pi^+}(W), \quad (2.3)$$

$$G(\Delta^2)=(1+3\propto_0)/(1+\propto_0)^3,$$

$$\propto_0=(\Delta^2+\mu^2)/[2m(m^*-m)].$$

Here $p^{\rm off}$ is the proton momentum in the initial state of the $p\pi^+$ system and m^* is the mass of the $N^*(1238)$. Jackson[10] has shown that a more rigorous derivation of this off-shell correction leads to $G(\Delta^2)\simeq1$. A recent calculation by Gutbrod[11] gives a result that is close to an average of the calculations of Ferrari-Selleri and Jackson. The influence of $G(\Delta^2)$ on the Δ^2 distribution will be examined later.

By fitting the ρ production data at 1.6 GeV/c,

[4] This value was obtained by interpolating the results of experiments at nearby energies. (See Refs. 2 and 3.)

[5] We fit the following function to the effective-mass distribution:

$$F(m,a,b,m_0,\Gamma)=\left[a+\frac{\frac{1}{2}b\Gamma}{(m-m_0)^2+\frac{1}{4}\Gamma^2}\right]\times{\rm PS},$$

where m stands for the effective mass and PS means the two-body ($p\pi^+$) phase space out of the four-body ($p\pi^+\pi^-\pi^-$) final state. m_0 is the central mass and Γ is the full width of the resonance. a and b are related to the percentage background and percentage resonance production, respectively.

[6] J. Alitti, J. P. Baton, A. Berthelot, B. Deler, W. J. Fickinger, N. Neveu-René, V. Alles-Borelli, R. Gessaroli, A. Romano, and P. Waloschek, Nuovo Cimento **35**, 1 (1965).

[7] F. Salzman and G. Salzman, Phys. Rev. **120**, 599 (1960).

[8] E. Ferrari and F. Selleri, Nuovo Cimento **21**, 1028 (1961); **24**, 453 (1962); **27**, 1450 (1963).

[9] The symbols are defined as follows: m is the mass of the proton, q_L is the incident lab momentum, V is the mass of the $\pi\pi$ system, q is the pion momentum in the $\pi\pi$ c.m. system, W is the mass of the $p\pi^+$ system; p is the proton momentum in the $p\pi^+$ c.m. system; μ is the mass of the pion.

[10] J. D. Jackson, Nuovo Cimento **36**, 1644 (1964).

[11] F. Gutbrod, Nuovo Cimento **45A**, 830 (1966).

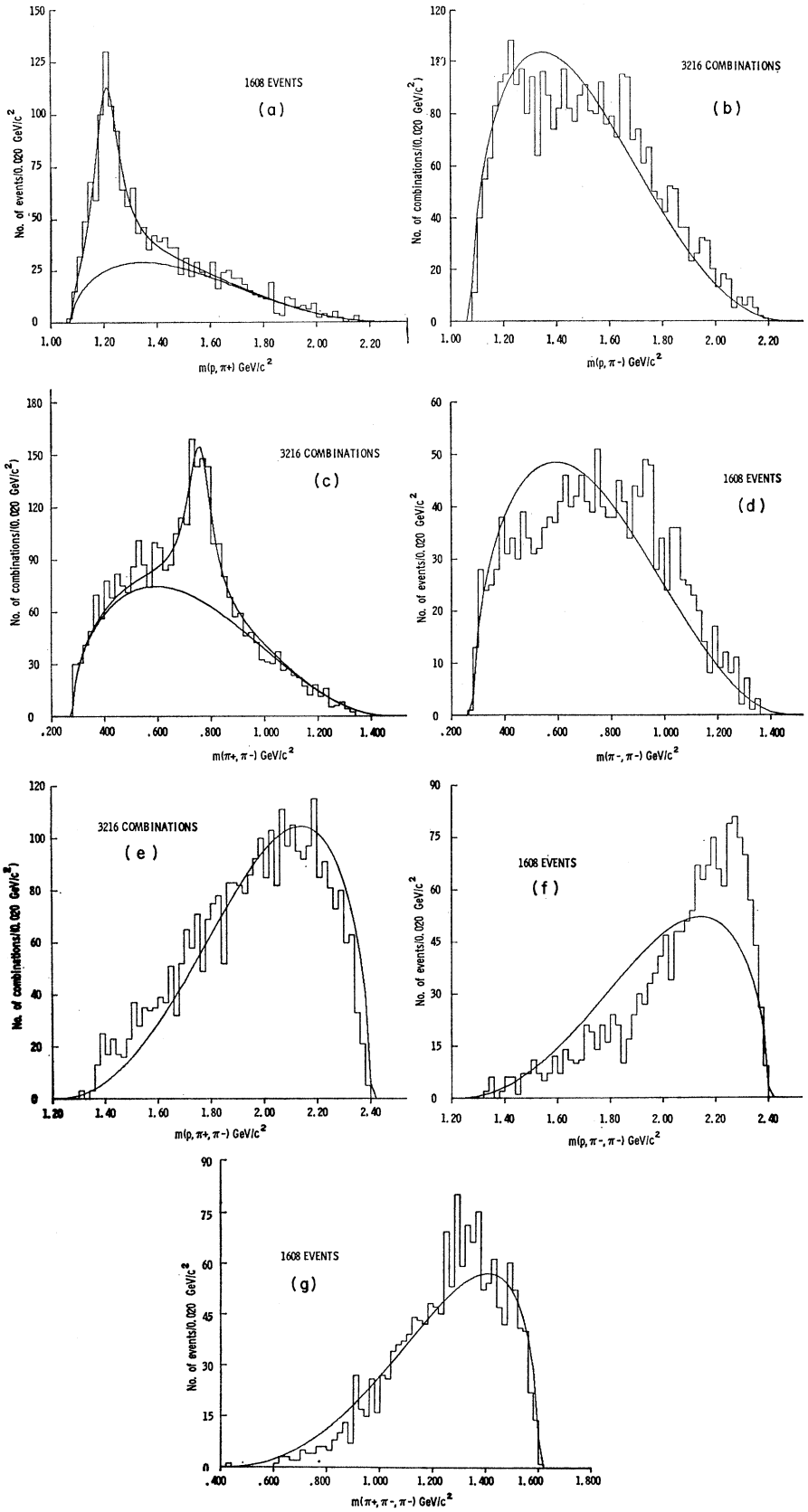

FIG. 1. Effective-mass distributions for all possible particle combinations in $\pi^- p \rightarrow p\pi^-\pi^+\pi^-$. (a) $p\pi^+$, (b) $p\pi^-$, (c) $\pi^+\pi^-$, (d) $\pi^-\pi^-$, (e) $p\pi^+\pi^-$, (f) $p\pi^-\pi^-$, (g) $\pi^+\pi^-\pi^-$. The solid curves are phase space, normalized to total events, except for 1(a) and 1(c), where phase space is multiplied by a constant plus a Breit-Wigner resonance form.

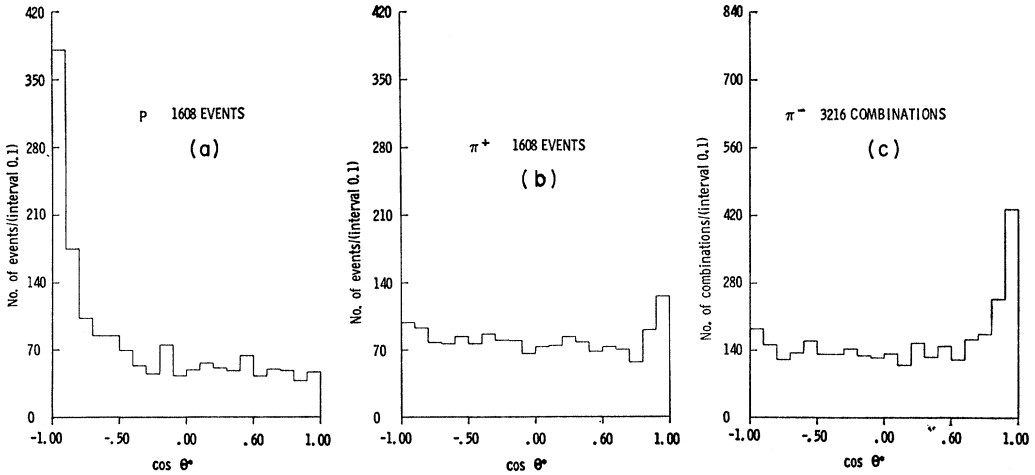

FIG. 2. Center-of-mass production angular distributions for all particles in $\pi^- p \to p\pi^-\pi^+\pi^-$. (a) p, (b) π^+, (c) π^- (multiplicity 2).

Amaldi and Selleri (AS)[12] determined a form factor

$$F(\Delta^2) = (0.72)/[1+(\Delta^2+\mu^2)/4.73\mu^2] + 0.28/\{1+[(\Delta^2+\mu^2)/32\mu^2]^2\}. \quad (2.4)$$

The OPE model with this form factor is known to give an adequate description of ρ production data at all incident energies. It is hoped then that the same form factor can be used to describe the process $\pi N \to N^*\pi\pi$.

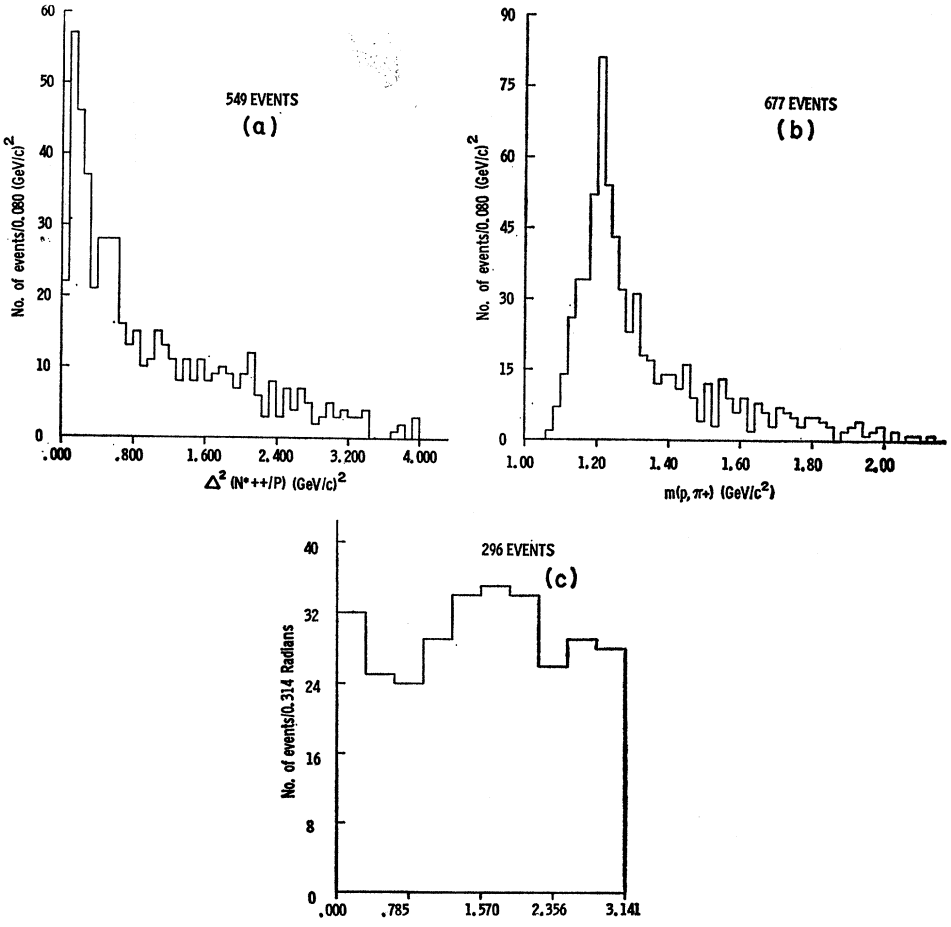

FIG. 3. (a) 4-momentum transfer squared from proton to $(p\pi^+)$ combinations, satisfying $1.16 < m(p\pi^+) < 1.28$ GeV/c^2; (b) $m(p\pi^+)$ for events with $\Delta^2(p\pi^+/p) < 0.8$ (GeV/c)^2; (c) Treiman-Yang angular distribution at N^{*++} vertex, i.e., for events with $1.16 < m(p\pi^+) < 1.28$ GeV/c^2 and $\Delta^2(p\pi^+/p) < 0.8$ (GeV/c)^2.

[12] U. Amaldi and F. Selleri, Nuovo Cimento 31, 360 (1964).

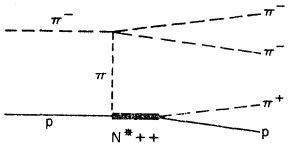

FIG. 4. Feynman diagram for process $\pi^- p \to N^{*++}\pi^-\pi^-$ via π exchange.

Equation (2.1) then becomes

$$(d^3\sigma)/(d\Delta^2 dW^2 dV^2) = |F(\Delta^2)|^2 |G(\Delta^2)|^2 H \times(\Delta^2, W^2, V^2, q_L)\sigma_{\pi\pi}(V), \quad (2.5)$$

where

$$H(\Delta^2, W^2, V^2, q_L) = \left(\frac{1}{16\pi^3}\right)\left(\frac{1}{m^2 q_L^2}\right)\left[\frac{1}{(\Delta^2+\mu^2)^2}\right] 2V^2 q \times\left(\frac{q^{\text{off}}}{q}\right)^{2l} W p \left(\frac{p^{\text{off}}}{p}\right)^2 \left[1+\frac{\Delta^2+\mu^2}{4m^2}\right]\sigma_{p\pi^+}(W^2).$$

Before this formula is applied to the $I=2$ s-wave $\pi\pi$ scattering, it is important to determine if it can give an adequate description of a similar process whose behavior is well known. Such a process is readily available in $\pi^- p \to N^{*0}(1238)\pi^+\pi^-$, where $\pi^+\pi^-$ resonates to produce ρ^0. In order to study this process, N^{*++} events with $1.11 < m(p\pi^+) < 1.32$ GeV/c^2 and $\Delta^2 < 1.8$ (GeV/c)^2 were excluded, and N^{*0} events with $1.12 < m(p\pi^-) < 1.30$ GeV/c^2, $\Delta^2 < 0.4$ (GeV/c)^2 were selected.

The resulting $m(\pi^+\pi^-)$ distribution is then compared with Eq. (2.5) integrated over W^2 and Δ^2 to yield $\sigma_{\pi^+\pi^-}(V)$. The integration is performed for p-wave scattering ($l=1$) with $G(\Delta^2)=1$ and the AS form factor. The cross section thus obtained is shown in Fig. 5.

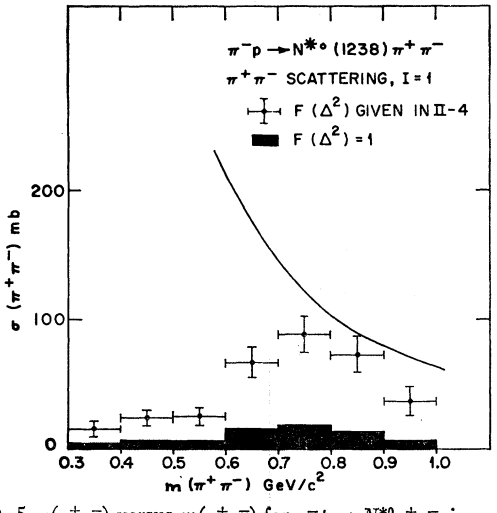

FIG. 5. $\sigma(\pi^+\pi^-)$ versus $m(\pi^+\pi^-)$ for $\pi^- p \to N^{*0}\pi^+\pi^-$, i.e., events with $1.11 < m(p\pi^+) < 1.32$ GeV/c^2 and $\Delta^2(p\pi^+/p) < 1.8$ (GeV/c)^2 excluded and events with $1.12 < m(p\pi^-) < 1.30$ GeV/c^2 and $\Delta^2(p\pi^-/p) < 0.4$ (GeV/c)^2 included. The solid line gives the unitarity limit 12 $\pi\lambda^2$. Points with error bars were obtained by integrating (2.5) over W^2 and Δ^2, with $F(\Delta^2)$ given by (2.4). Points ■ were obtained by integrating (2.5) over W^2 and Δ^2, with $F(\Delta^2)=1$.

The solid line in the figure is the p-wave unitarity limit $12\pi\lambda^2$. The cross section obtained with $F(\Delta^2)=1$ is indicated by the shaded area. It is obvious that the latter choice of form factor cannot describe the resonant $\pi^+\pi^-$ scattering near ρ^0. On the other hand, the OPE model with the AS form factor appears to give a satisfactory description of this process, especially in view of the complicated selections applied to a channel with a multiplicity of two.

This analysis is now applied to the $\pi^-\pi^-$ scattering process. Figure 6(a) gives the observed $m(\pi^-\pi^-)$ distribution for the N^{*++} events [$1.16 < m(p\pi^+) < 1.28$ GeV/c^2] with $\Delta^2 < 0.8$ (GeV/c)^2. The shaded area represents those events with $\Delta^2 < 0.4$ (GeV/c)^2 which were used in the following analysis. The $\pi\pi$ scattering angle is plotted against $m(\pi\pi)$ in Fig. 6(b). The scattering is mostly isotropic up to a $m(\pi\pi)$ value of 0.8 GeV/c^2. The forward peaking in the $\pi\pi$ angular distribution beyond 0.8 GeV/c^2 may be due to a constructive interference of s and d waves.

Integration over Δ^2 and W^2 of Eq. (2.5) is performed with $l=0$, $G(\Delta^2)=1$, and the AS form factor. $\Delta^2 < 0.4$ (GeV/c)^2 and $1.16 < W < 1.28$ GeV/c^2 were used as appropriate limits. The result of the $I=2$ $\pi\pi$ scattering cross-section reduction is tabulated in Table I and plotted in Fig. 7. If instead of Jackson's formula, the Ferrari-Selleri form for the off-shell $\sigma_{p\pi^+}$ corrections had been used, the calculated cross sections would have been higher by percentages ranging from 14% at the lowest $m(\pi)$ bin (0.3–0.5 GeV/c^2) to 80% at the highest $m(\pi\pi)$ bin (0.9–1.0 GeV/c^2). The use of Gutbrod's formula would result in cross sections lying half-way between the above two results.

An earlier analysis by Schmitz[13] of $I=2$ $\pi\pi$ scattering using $\pi^- p \to N^{*++}\pi^-\pi^-$ at 4 GeV/c was done using the Salzman-Salzman formula. This is almost equivalent to setting $F(\Delta^2)=1$ and $G(\Delta^2)=1$ in Eq. (2.5). The cross sections thus obtained are much smaller than the present results (by a factor ranging from 2 to 5). This discrepancy is due entirely to the different choice of $F(\Delta^2)$.

A similar analysis by Alitti *et al.*[6] using $\pi^- p \to N^{*++}\pi^-\pi^-$ at 2.75 GeV/c also results in lower cross sections. The formula used in their work is equivalent to Eq. (2.5) with $F(\Delta^2)=1$, and the Ferrari-Selleri form of $G(\Delta^2)$. Results similar to those of Alitti *et al.* were obtained by Armenise *et al.*,[14] who used a Chew-Low equation to analyze the reaction $\pi^+ p \to n\pi^+\pi^+$ at 2.75 GeV/c.

The ABBBHLM collaboration[3] made an analysis of $\pi^+ p \to n\pi^+\pi^+$ at 4 GeV/c using a variety of methods: the Chew-Low formula for s-wave $\pi\pi$ scattering, the Selleri formula for s-wave $\pi\pi$ scattering, and the Selleri

[13] N. Schmitz, Nuovo Cimento **31**, 255 (1964).
[14] N. Armenise, B. Ghidini, S. Mongelli, A. Romano, P. Waloschek, J. Laberrigue-Frolow, Nguyen Hun Khanh, C. Ouannes, M. Sene, and L. Vigneron, Nuovo Cimento **37**, 361 (1965).

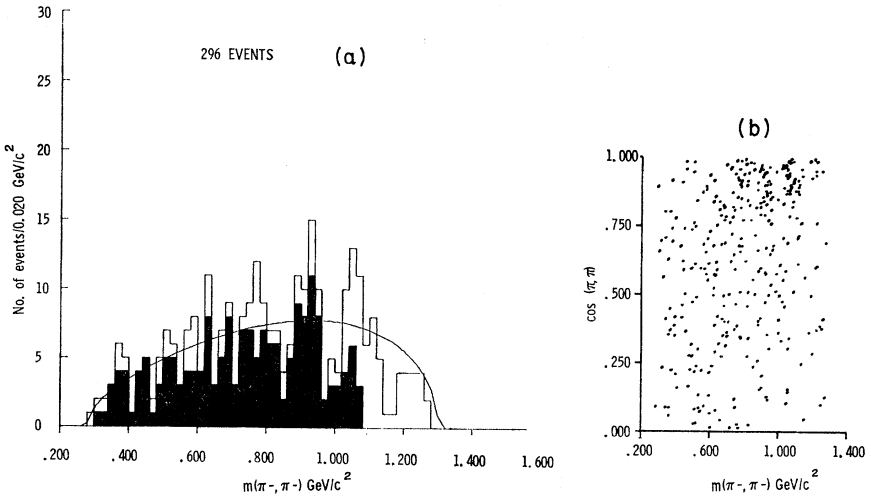

FIG. 6. (a) $m(\pi^-\pi^-)$ for events with $1.16<m(p\pi^+)<1.28$ GeV/c^2 and unshaded area $\Delta^2<0.8$ (GeV/c)^2; shaded area, $\Delta^2<0.4$ (GeV/c)^2. The solid line is the $\pi\pi$ phase space for the process $\pi^-p\to N^{*++}\pi^-\pi^-$ normalized to all events with $\Delta^2<0.8$ (GeV/c)^2. (b) Scatter plot of $m(\pi^-\pi^-)$ versus $\pi\pi$ scattering angle for events with $1.16<m(p\pi^+)<1.28$ GeV/c^2 and $\Delta^2(p\pi^+/p)<0.8$ (GeV/c)^2.

formula for d-wave $\pi\pi$ scattering. Use of the Chew-Low formula gives results similar to that of Armenise *et al.* The use of the Selleri formula for s-wave scattering gives a result comparable to the one obtained in the present work. This result is also plotted in Fig. 7.[15] Agreement between the two results is quite reasonable.

It is of some interest to find out if the OPE model with the form factor given by Eq. (2.5) can give a reasonable description of the Δ^2 distribution. The two most populous bins of $m(\pi^-\pi^-)$ were chosen and the $\Delta^2(\pi^-\pi^-)$ distributions for each were compared to those given by Eq. (2.5), evaluated using the AS form factor. The result is given in Figs. 8(a) and 8(b). The lower solid lines are computed with $G(\Delta^2)=1$, and the upper solid lines with the Ferrari-Selleri off-shell correction. (These curves are not normalized to the total number of events.) Either of these curves could fit the experimental distribution reasonably well. The choice of $F(\Delta^2)=1$ and $G(\Delta^2)=1$ was found to be inconsistent with the experimental distributions, whereas $F(\Delta^2)=1$ and $G(\Delta^2)$ as given by Eq. (2.3) produced curves similar in shape to the upper curves, but with an absolute magnitude higher by a factor of approximately 3.

Walker *et al.*[16] analyzed a number of experimental results for the reactions $\pi^\pm p\to\pi\pi N$ to obtain the s-wave $\pi\pi$ phase shifts for $I=0$ and $I=2$ states. Their values of the $I=2$ phase shifts are in reasonable agreement with the present results below about 700 MeV in $m(\pi^-\pi^-)$. Part of the disagreement above 700 MeV can be attributed to the contamination of the present $\pi\pi$ sample due to background $\pi^-p\to N^{*0}\rho^0$ events. Although the total contamination due to this source is estimated to be less than 20%, most of these are concentrated at the higher $\pi\pi$ mass region. The present results are compared with those of Walker *et al.* in Fig. 9.

The $\pi\pi$ scattering length a_2^0 as obtained from the effective-range formalism was found to be

$$|a_2^0|=0.19m_\pi^{-1}.$$

The statistical error in the above estimate is about 12%.

TABLE I. $I=2$ $\pi\pi$ scattering cross section results.

$m(\pi\pi)$ (GeV/c^2)	k^2 (10^{26} cm^{-2})	No. of events	$(d\sigma/dV^2)\Delta V^2$ (μb)	$\sigma(\pi\pi)$ (mb)	Unitary limit $8\pi\lambda^2$ (mb)
0.3–0.5	0.51	27	30.2	19.6±3.7	513
0.5–0.6	1.44	23	25.8	17.8±3.7	175
0.6–0.7	2.21	28	31.4	17.8±3.4	114
0.7–0.8	3.11	29	32.5	17.3±3.3	81
0.8–0.9	4.14	27	30.2	17.1±3.3	61
0.9–1.0	5.30	32	35.8	24.4±4.2	47

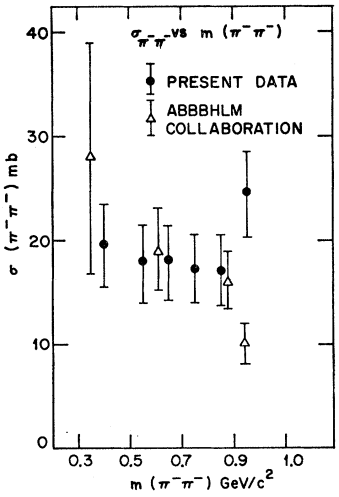

FIG. 7. $I=2$ $\pi\pi$ scattering cross section obtained by integrating (2.5) over Δ^2 and W^2 for $l=0$, $G(\Delta^2)=1$ and $F(\Delta^2)$ of (2.4) for events with $1.16<m(p\pi^+)<1.28$ and $\Delta^2<0.4$. ● present data; △ ABBBHLM data up to 1 GeV/c in $m(\pi^-\pi^-)$.

[15] Only their results up to 1 GeV/c in $m(\pi\pi)$ are used here.

[16] W. D. Walker, J. Carroll, A. Garfinkel, and B. Y. Oh, Phys. Rev. Letters 18, 630 (1967).

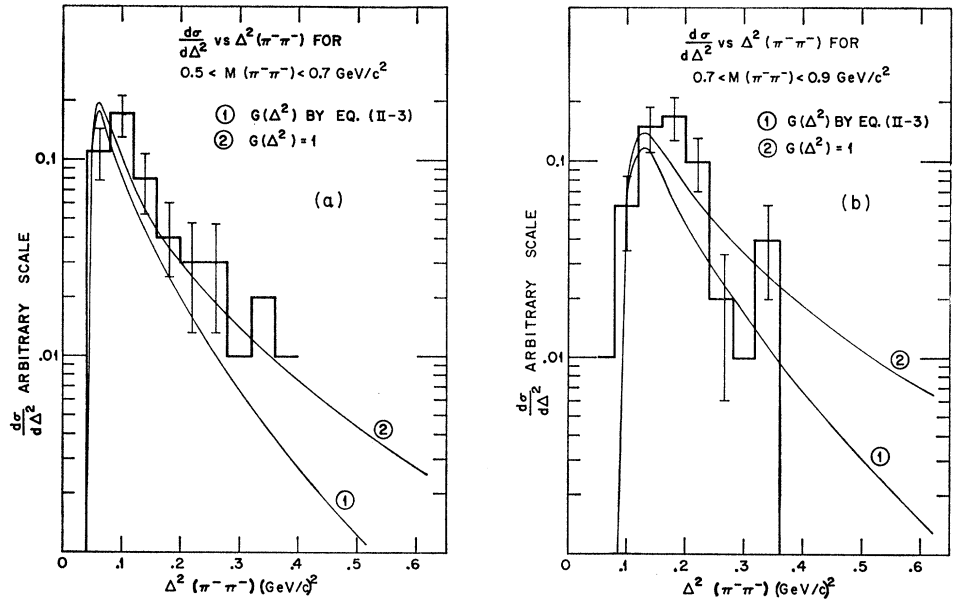

FIG. 8. (a) $d\sigma/d\Delta^2$ versus $\Delta^2(\pi^-\pi)$ [i.e., 4-momentum transfer from incident π to $(\pi^-\pi^-)$ pair] for events with $1.16<m(p\pi^+)<1.28$ GeV/c^2 and $0.5<m(\pi^-\pi^-)<0.7$ GeV/c^2. The solid curves were calculated with $F(\Delta^2)$ of (2.4) and (1) with $G(\Delta^2)$ of (2.3), (2) with $G(\Delta^2)=1$. (b) Same as (a) with $0.7<m(\pi^-\pi^-)<0.9$ GeV/c^2.

However, the systematic errors due to the uncertainties in the OPE model used for this analysis and the uncertainties in the background contamination are certainly larger than this.

There is a number of theoretical calculations on a_2 and a_0. Brandsen and Moffat[17] used dispersion relations to obtain $a_2=+0.21m_\pi^{-1}$ and $a_0=0.67$ m_π^{-1}. Weinberg[18] used a current-algebra approach to obtain $a_2=-0.06$ m_π^{-1} and $a_0=0.20$ m_π^{-1}.

Although the present result favors the calculation of Brandsen and Moffat, the large systematic uncertainties make it impossible to rule out Weinberg's result.

B. ρ^0 and N^{*0} Production

A BW fit to the $\pi^+\pi^-$ invariant mass distribution of Fig. 1(c) gave the following results:

Percentage of ρ^0	$(40\pm5)\%$
Central mass	760 ± 5 MeV/c
Width	113 ± 16 MeV/c.

Isobar production in the $p\pi^-$ combination is considerably weaker than either N^{*++} or ρ^0 production. The reflection of N^{*++} and the double multiplicity complicates the analysis of this channel. The $p\pi^-$ combination with lower $\Delta^2(p\pi^-)$ is plotted in Fig. 10, where

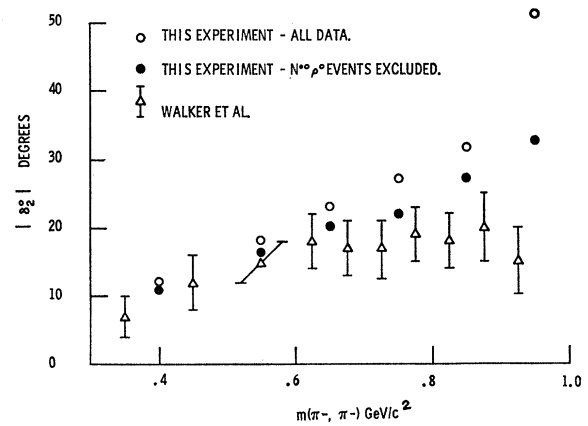

FIG. 9. $m(\pi^-\pi^-)$ versus $I=2$ s-wave $\pi\pi$ phase shift. The statistical errors for the results of the present experiment, which are typically of the order of 10%, have not been indicated.

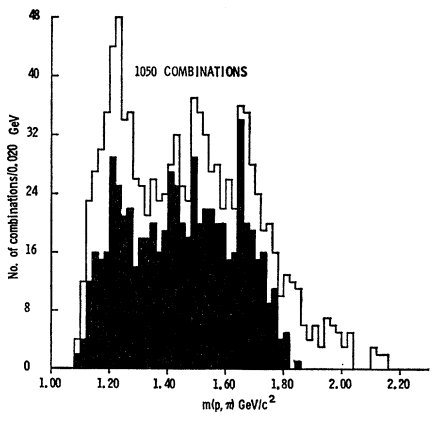

FIG. 10. The unshaded area shows $m(p\pi^-)$ for $\pi^-p\to p\pi^-\pi^+\pi^-$ where the $p\pi^-$ combination with the lower $\Delta^2(p\pi^-/p)$ is chosen, and events with $1.12<m(p\pi^+)<1.32$ GeV/c and $\Delta(p\pi^+/p)<1.5$ (GeV/c)^2 are excluded. The shaded area shows $m(p\pi^-_1)$ for $\pi^-p\to p\pi^-_1\pi^+\pi^-_2$ where $(\pi^+\pi^-_2)$ lies in $0.66<m(\pi^+\pi^-_2)<0.84$ GeV/c^2 and events with $1.12<m(p\pi^+)<1.32$ GeV/c^2 and $\Delta^2(p\pi^+/p)<1.5$ (GeV/c)^2 excluded. If both $\pi^+\pi^-_1$ and $\pi^+\pi^-_2$ lie in ρ band, the $(p\pi^-)$ combination with lower $\Delta^2(p\pi^-/p)$ is plotted.

[17] B. H. Brandsen and J. W. Moffat, Nuovo Cimento **21**, 505 (1961).
[18] S. Weinberg, Phys. Rev. Letters **17**, 616 (1966).

N^{*++} events ($1.12<m(p\pi^+)<1.32$ GeV/c^2 and $\Delta^2(p\pi^+)<1.5$ (GeV/c)^2 have been removed. $N^{*0}(1238)$, $N^{*0}(1400)$, $N^{*0}(1525)$, and $N^{*0}(1688)$ productions are seen. The N^{*0}'s are produced predominantly together with $\rho^0(760)$, as can be seen from the shaded histogram of Fig. 10. Here, in addition to the N^{*++} and Δ^2 cuts mentioned above, $m(p\pi^-)$ is plotted only if the other π^- satisfies $0.66<(\pi^+\pi^-)<0.84$ GeV/c^2.

The production of ρ^0 has long been assumed to proceed via OPE. In fact, the absorption model of Gottfried and Jackson[19] has been shown to give a satisfactory description of the decay angular correlations in a similar process $\pi^+p\rightarrow N^{*++}\rho^0$ at various incident energies. The OPE model with a form factor was shown in Sec. IIA to give the right order of magnitude for the $\pi^-p\rightarrow N^{*0}(1238)\rho^0$ cross section.

The ρ region is defined henceforth as $0.66<m(\pi^+\pi^-)<0.84$ GeV/c^2; for purposes of comparison two control regions above and below the ρ region are defined as $0.84<m(\pi^+\pi^-)<1.1$ GeV/c^2 and $0.40<m(\pi^+\pi^-)<0.66$ GeV/c^2. Some ambiguity arises from events in which both $\pi^+\pi^-$ combinations lie in the mass region considered. For the purposes of plotting the various angular distributions considered below, two points are plotted for each event of this type. The following results are not materially affected by the use of other possible methods of treating this ambiguity.

Figure 11 shows the c.m. production angle with respect to the incident π^- for the $\pi^+\pi^-$ combinations in the three regions defined above. The extremely strong forward peaking for the events in the ρ^0 region indicates that the ρ^0 is produced peripherally. This conclusion is supported by a study of the $\Delta^2(\pi^+\pi^-)$ spectra for the three regions, and the $\pi^+\pi^-$ invariant-mass distribution for events with $\Delta^2(\pi^+\pi^-)<0.5$ (GeV/c)^2.

These observations suggest that the OPE mechanism

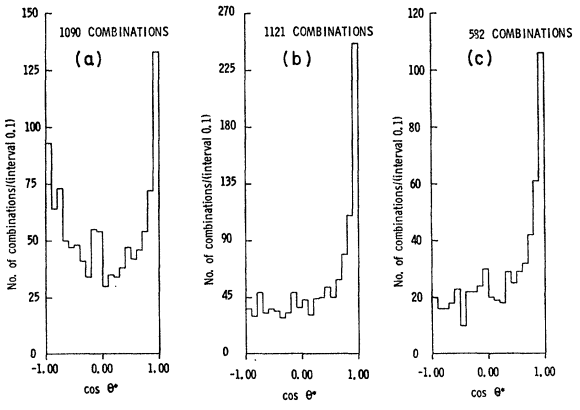

FIG. 11. Center-of-mass production angles for $\pi^+\pi^-$ combinations [i.e., cos $(\pi^-_{\text{in}}, (\pi^+\pi^-)_{\text{out}})$] with (a) $m(\pi^+\pi^-)$ in 0.4–0.66 GeV/c^2, (b) $m(\pi^+\pi^-)$ in 0.66–0.84 GeV/c^2, (c) $m(\pi^+\pi^-)$ in 0.84–1.1 GeV/c^2.

[19] K. Gottfried and J. D. Jackson, Nuovo Cimento **34**, 735 (1964); J. D. Jackson, J. T. Donohue, K. Gottfried, R. Keyser, and B. E. Y. Svensson, Phys. Rev. **139**, B428 (1965).

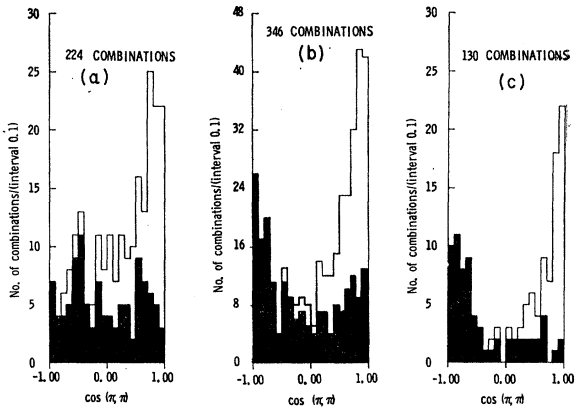

FIG. 12. The unshaded area shows the cosine of the π^- scattering angle—i.e., cos$(\pi^-_{\text{in}}, \pi^-_{\text{out}})$ in the $(\pi^+\pi^-)$ c.m. system a for $m(\pi^+\pi^-)$ in 0.4–0.66 GeV/c^2, (b) for $m(\pi^+\pi^-)$ in 0.66–0.84 GeV/c^2, (c) for $m(\pi^+\pi^-)$ in 0.84–1.1 GeV/c^2, all for events with $\Delta^2(\pi^+\pi^-/\pi^-)<0.5$ (GeV/c)^2. The shaded area is the as above with N^{*++} events excluded [i.e., those with $1.12<m(p\pi^+)<1.32$ GeV/c^2].

may be responsible for ρ^0 production at low values of $\Delta^2(\pi^+\pi^-)$. The π^- scattering angle in the $\pi^+\pi^-$ rest system is shown in Fig. 12 for the three mass regions, for events having $\Delta^2(\pi^+\pi^-)<0.5$ (GeV/c)^2. The isotropy of the Treiman-Yang angle distributions and the presence of a strong cos^2 dependence in the scattering angle distributions is in qualitative agreement with the predictions of the OPE model, as observed in other studies of this channel. The values of the asymmetry parameter $R=(F-B)/(F+B)$ for the scattering angle distribution for the different mass regions are listed in Table II. These values are lower than those obtained for the reaction $\pi^-p\rightarrow\rho^0n$ in the same exposure.[1] The competing N^{*++} channel has a strong effect on all these angular distributions, as may be seen in Fig. 12, where the shaded histograms represent events for which, in addition to the $\Delta^2(\pi^+\pi^-)$ cut, the $p\pi^+$ invariant mass lies outside the region $1.12<m(p\pi^+)<1.32$ GeV/c^2. The values of R quoted in Table II are thus considered as upper limits.

C. The A Mesons

(a) The enhancement around 1300 MeV in the 3π invariant mass spectrum shown in Fig. 1(g) is attributed to the A_2 meson. In order to reduce the background, the competing N^{*++} channel has been removed by excluding those events with $1.12m(p\pi^+)<1.32$ GeV/c^2 which have $\Delta^2(p\pi^+)<1.5$ (GeV/c)^2. As may be seen from the shaded

TABLE II. Asymmetry parameters in the ρ^0 mass region.

$m(\pi^+\pi^-)$ region (GeV/c^2)	$R=(F-B)/(F+B)$
0.4 –0.66	0.30±0.07
0.66±0.84	0.28±0.06
0.84–1.1	0.22±0.09

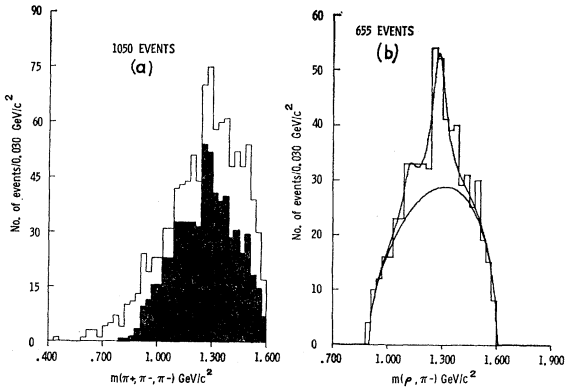

FIG. 13. (a) $m(\pi^+\pi^-\pi^-)$ with events with $1.12<m(p\pi^+)<1.32$ GeV/c^2 and $\Delta^2(p\pi^+/p)<1.5$ (GeV/c)^2 excluded. The shaded histogram represents events with at least one $\pi^+\pi^-$ combination in $0.66<m(\pi^+\pi^-)<0.84$ GeV/c^2. (b) The shaded histogram in (a), fitted to Breit-Wigner and phase-space distributions.

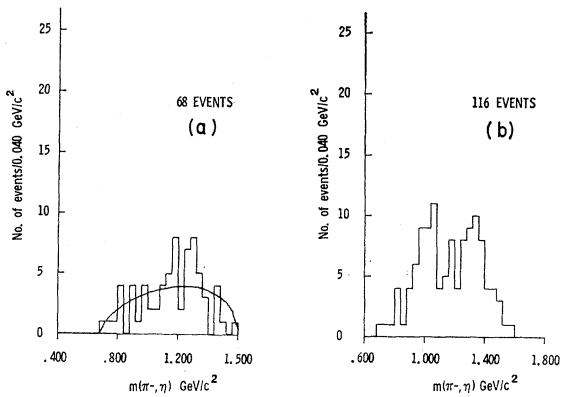

FIG. 14. (a) $m(\pi^-\pi^+\pi^-\pi^0)$ for $\pi^-p\to\pi^-p\pi^+\pi^-\pi^0$ with $0.53<m(\pi^+\pi^-\pi^0)<0.56$ GeV/c^2. (The solid line is the phase-space distribution normalized to all events.) (b) $m(\pi^-x)$ for $\pi^-p\to\pi^-px$ with $0.500<m(x)<0.600$ GeV/c^2, where x means missing neutral particle(s).

portion of Fig. 13(a), the A_2 peak is undiminished by selecting only those events which have at least one $\pi^+\pi^-$ combination in the ρ region (0.66–0.84 GeV/c^2), indicating that the 3π decay of the A_2 proceeds almost entirely through $\rho\pi$, in agreement with previous results. The $\rho\pi^-$ spectrum also shows a shoulder around 1100 MeV, usually called the A_1 meson. In Fig. 13(b), the $\rho\pi$ distribution (N^{*++} events with small Δ^2 removed) has been fitted to phase space plus two BW resonance curves, as described earlier. This fit yields the values for the mass and width of the two A mesons given in Table III.

A search for the observed[20] $\pi\eta$ decay mode of the A_2 meson was made in the channels $\pi^-p\pi^+\pi^-\pi^0$ and π^-p + (missing mass) [i.e., no fit events with missing mass greater than $m(\pi^0)$]. In the $\pi^-p\pi^+\pi^-\pi^0$ final state the η was defined by $530<m(\pi^+\pi^-\pi^0)<560$ MeV/c^2 and, for the two-prong missing mass events, a slightly broader η ($500<$missing mass<600 MeV/c^2) was chosen to take into account the poorer resolution in this channel. The results are shown in Figs. 14(a) and 14(b). An enhancement is observed above phase space around 1.0 GeV/c^2 in the π^-n (missing) spectrum but none in the $\pi^-\eta$ (visible) spectrum, but it is not clear whether this enhancement is related to the A_1.

TABLE III. Fitted parameters for A_1 and A_2 mesons.

Meson	Mass (MeV/c^2)	Width (MeV/c^2)	Percentage of channel $\rho\pi^+\pi^-\pi^-$
A_1	1119±30	76±46	1.7±1.3
A_2	1280±12	91±18	7.0±1.9

[20] J. Alitti, J. P. Baton, B. Deler, M. Neveu-René, J. Crussard, J. Ginestet, A. H. Tran, R. Gessaroli, and A. Romano, Phys. Letters **15**, 69 (1965); M. S. Dubovikov, V. K. Grogoryev, A. P. Grishin, V. M. Guzhavin, G. K. Kliger, V. Z. Kolganov, A. V. Lebedev, G. S. Lomkatsi, Yu. A. Simonov, V. T. Smolyankin, A. P. Sokolov, G. D. Tikhomirov, K. A. Trostina, I. A. Vetlitsky, V. V. Vladimirsky, and I. A. Yerofeev, *ibid.* **23**, 716 (1966).

This accumulation of events at the lower end of the $\pi^-\eta$ (missing) spectrum makes difficult the estimation of phase space. However, using a reasonable free-hand fit, the number of events in the A_2 region is consistent with the accepted branching ratio.[21]

$$[\eta\to(\pi^+\pi^-\pi^0+\pi^+\pi^-\gamma)]/(\eta\to\text{ all neutrals})\simeq 0.37.$$

Using this value for the η branching ratio, and assuming that

$$(A_2^-\to\rho^0\pi^-)/(A_2^-\to\rho^-\pi^0)=1,$$

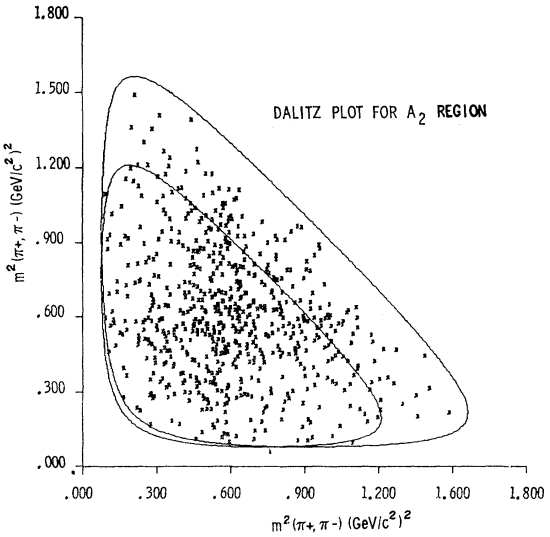

FIG. 15. Dalitz plot for events in $1.24<m(\pi^+\pi^-\pi^-)<1.39$ GeV/c^2 with events $1.12<m(p\pi^+)<1.32$ GeV/c^2 and $\Delta^2(p\pi^+/p)<1.5$ (GeV/c)^2 excluded. Each event is plotted twice. The solid lines indicate kinematic limits for $m(\pi^+\pi^-\pi^-)=1.24$ and 1.39 GeV/c^2.

[21] A. H. Rosenfeld, A. Barbaro-Galtieri, W. J. Podolsky, L. R. Price, P. Soding, C. G. Wohl, M. Roos, and W. J. Willis, Rev. Mod. Phys. **39**, 1 (1967).

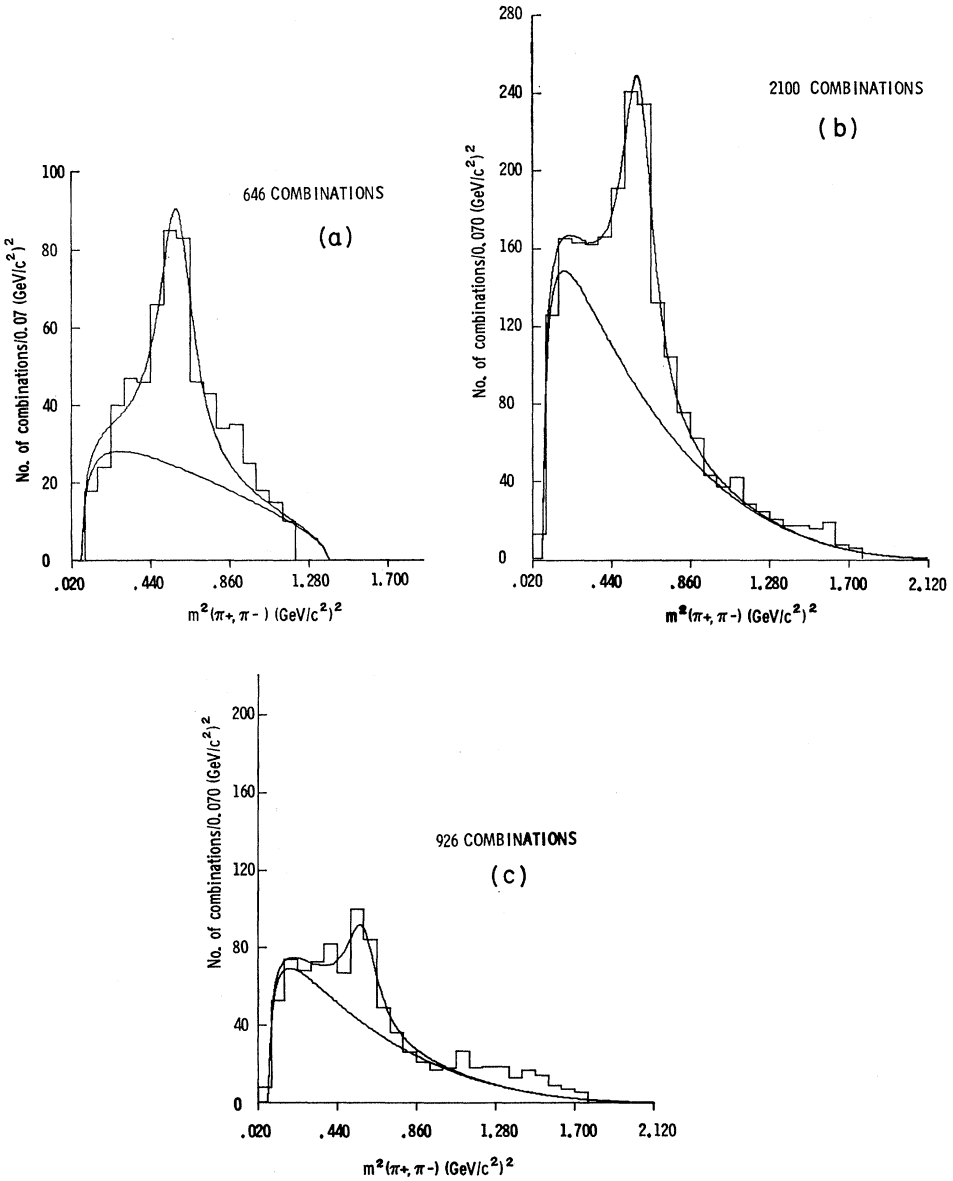

FIG. 16. Events with $1.12<m(p\pi^+)<1.32$ GeV/c^2 and $\Delta^2(p\pi^+/p)<1.5$ (GeV/c)^2 removed. (a) $m^2(\pi^+\pi^-)$ for $1.24<m(\pi^+\pi^-\pi^-)<1.39$ GeV/c^2; (b) $m^2(\pi^+\pi^-)$ for all events (after N^{*++} and Δ^2 cuts); (c) $m^2(\pi^+\pi^-)$ for events with $m^2(\pi^+\pi^-\pi^-)$ outside 1.09 to 1.39 GeV/c^2. The solid lines in these plots show phase-space and Breit-Wigner curves.

the result

$$(A_2^- \to \eta\pi)/(A_2^- \to \rho\pi)=0.16\pm0.10$$

is obtained.

(b) There has been considerable discussion as to whether the A_1 is a genuine resonance or the result of a kinematic enhancement.[22] The weak statistical significance of the A_1 enhancement and the strong dependence of the results on the method of analysis make it impossible to reach any conclusion from the present data.

(c) A method described by Frazer, Fulco, and Halpern,[23] for determining the A_2 spin and parity has been applied to the present data. In the analysis, N^{*++} events with $\Delta^2<1.5$ (GeV/c)^2 have been removed; the calculation has been repeated with exclusion of all N^{*++} events, and the results are qualitatively unchanged. Henceforth the A_2 region is defined by $1.24<m(\pi^+\pi^-\pi^-)<1.39$ GeV, and the ρ band by $0.44<m^2(\pi^+\pi^-)<0.72$ (GeV/c^2)^2.

The expected distribution of the points in the ρ band of the Dalitz plot for the $(\pi^+\pi^-\pi^-)$ system in the A_2 region has been calculated by Frazer *et al.*[23] for spin values up to 2. In order to compare these theoretical predictions with experiment, it is necessary to know the background under the A_2 peak. A fit to the $(\rho\pi)$ phase

[22] R. T. Deck, Phys. Rev. Letters **13**, 169 (1964); U. Maor and T. A. O'Halloran, *ibid.* **15**, 281 (1965); G. Goldhaber and S. Goldhaber, University of California Radiation Laboratory Report No. UCRL-16744 (unpublished).

[23] W. R. Fraser, J. R. Fulco, and F. R. Halpern, Phys. Rev. **136**, B1207 (1964).

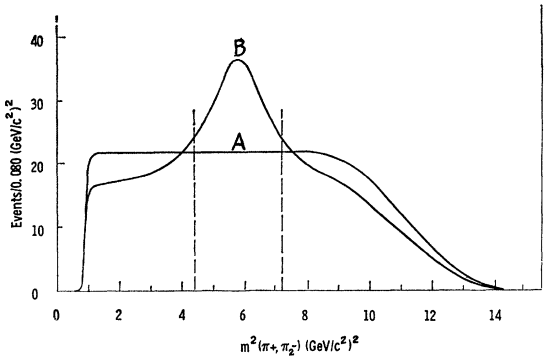

FIG. 17. Assumed forms of background in A_2 region for projection of ρ band of Dalitz plot. A—3π, B—$\rho\pi$.

space normalized to the number of events outside the A_1 and A_2 regions (1.09–1.39 GeV) leads to the estimate that $(66\pm6)\%$ of the events in the A_2 region of Fig. 13(b) are background, where the quoted error is statistical. The upper and lower limits on this total background (B) are taken to be $B=50\%$ and $B=80\%$, respectively.

In early analyses of the A_2 spin and parity, this background was usually not considered. However, allowance for the background contribution drastically alters the spin-parity assignments, as was shown, for example, by Benson *et al.*,[24] who assumed that the background was entirely 3π nonresonant in character.

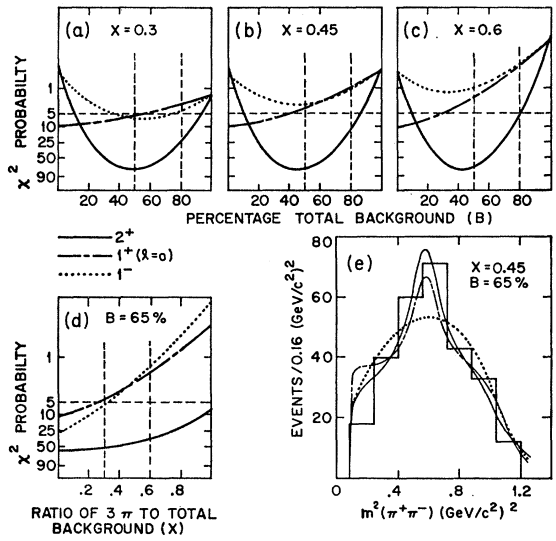

FIG. 18. χ^2 probability for 6 degrees of freedom for 2^+ (dash) $1^+(l=0)$ (dot-dash) and 1^- (dot) as a function of B with (a) $X=0.3$; (b) $X=0.45$; (c) $X=0.6$; and as a function of X with (d) $B=65\%$ ((the region of the plots above the horizontal dashed line is excluded at the 95% confidence level for six degrees of freedom and the vertical dashed lines indicate the limits of X and B); (e) projection of ρ band of Dalitz plot of Fig. 14 compared to theoretical predictions for 2^+, 1^+ ($l=0$), and 1^- with $X=0.45$ and $B=65\%$.

[24] G. Benson, L. Lovell, E. Marquit, B. Roe, D. Sinclair, and J. Vander Velde, Phys. Rev. Letters **16**, 1177 (1966).

However, the presence of directly produced ρ mesons (i.e., not arising from the decay of the A_2) may also contribute to the total background. This possibility was also considered by Chung *et al.*[25]

The ratio (X) of the 3π to total (i.e., 3π plus $\rho\pi$) background under the A_2 peak has been estimated in the following ways.

(i) The density of points in the Dalitz plot of Fig. 15 outside the ρ bands has been estimated. It is then assumed that this density, which can only come from the 3π component of the background, is constant over the entire Dalitz plot, and, in particular, throughout the ρ bands. The analysis is complicated by the fact that this Dalitz plot is a superposition of many such plots corresponding to 3π masses from 1.24 to 1.39 GeV. Uncertainty is also introduced by the fact that some $\rho\pi$ events coming from the tail of the ρ mass spectrum will also contribute to the area outside the ρ bands chosen. A value of $X\simeq0.44\pm0.15$ is obtained.[26]

(ii) The histogram of the $m^2(\pi^+\pi^-)$ spectrum for events in the region $(1.24<m(\pi^+\pi^-\pi^-)<1.39$, no ρ selection) is shown in Fig. 16(a). The number of events in the ρ peak $[0.44<m^2(\pi^+\pi^-)<0.72$ $(\mathrm{GeV}/c^2)^2]$ above background is estimated. This number includes events in which the ρ is produced from the A_2 meson decay. (It is assumed that none of the A_2 mesons decays

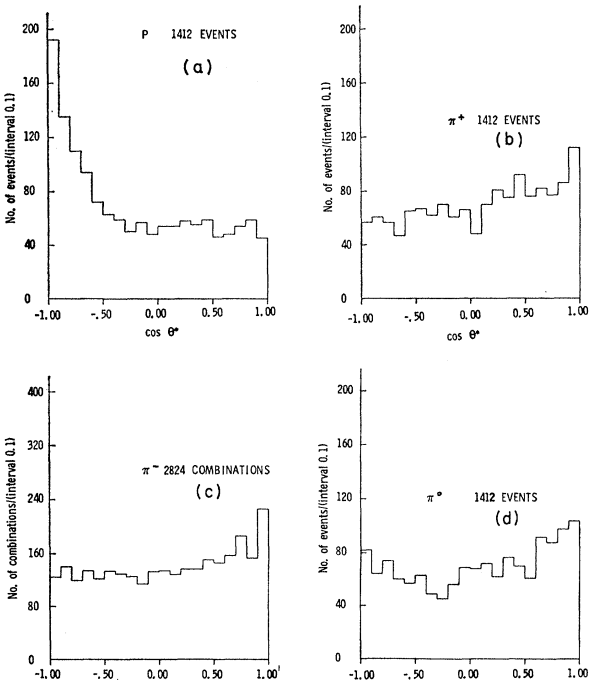

FIG. 19. Center-of-mass angular distributions for $\pi^-p\to\pi^-p\pi^+\pi^-\pi^0$: (a) proton, (b) π^+, (c) π^-, (d) π^0.

[25] Suh Urk Chung, O. I. Dahl, L. M. Hardy, R. I. Hess, J. Kirz, and D. H. Miller, Phys. Rev. Letters **18**, 100 (1967).

[26] The quoted errors in the values of X are estimated maximum deviations.

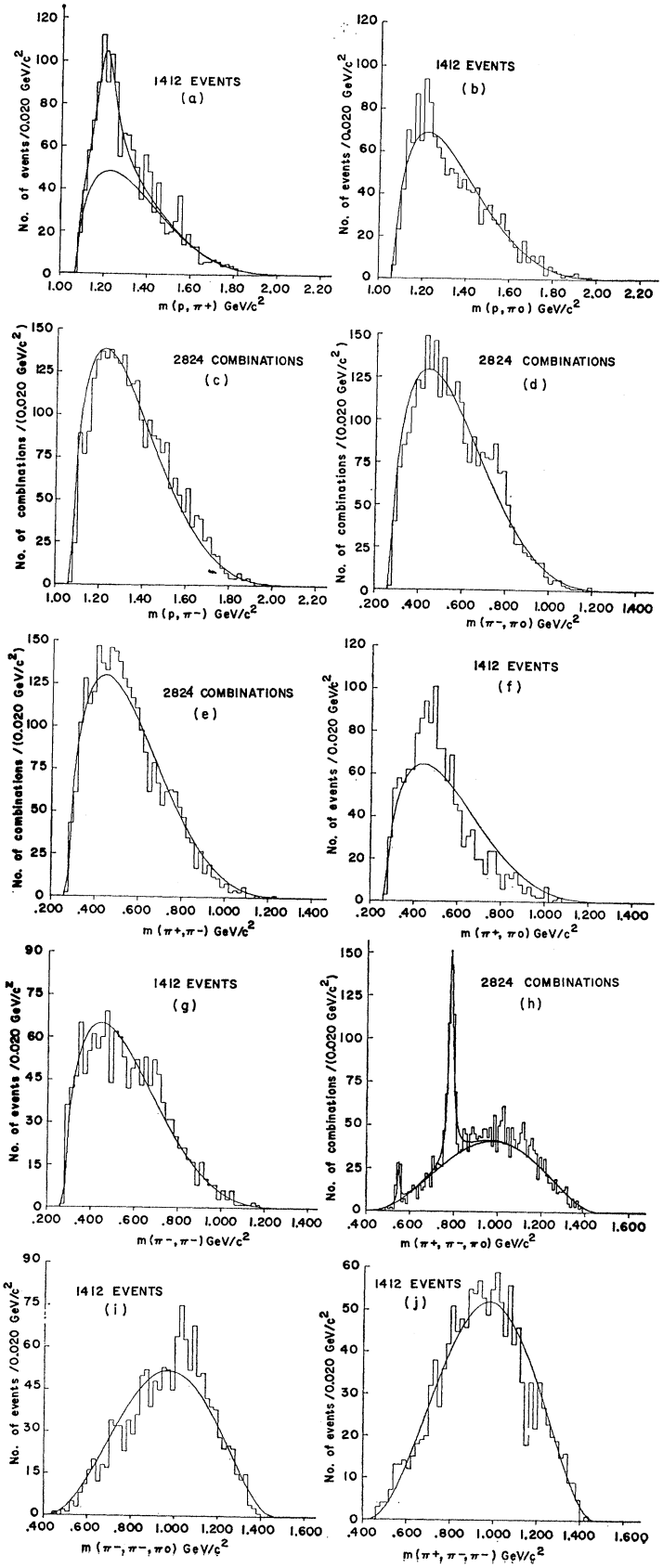

FIG. 20. Mass plots for $\pi^- p \to p\pi^+\pi^-\pi^-\pi^0$: (a) $p\pi^+$, (b) $p\pi^0$, (c) $p\pi^-$, (d) $\pi^-\pi^0$, (e) $\pi^+\pi^-$, (f) $\pi^+\pi^0$, (g) $\pi^-\pi^-$, (h) $\pi^+\pi^-\pi^0$, (i) $\pi^-\pi^-\pi^0$, (j) $\pi^+\pi^-\pi^-$.

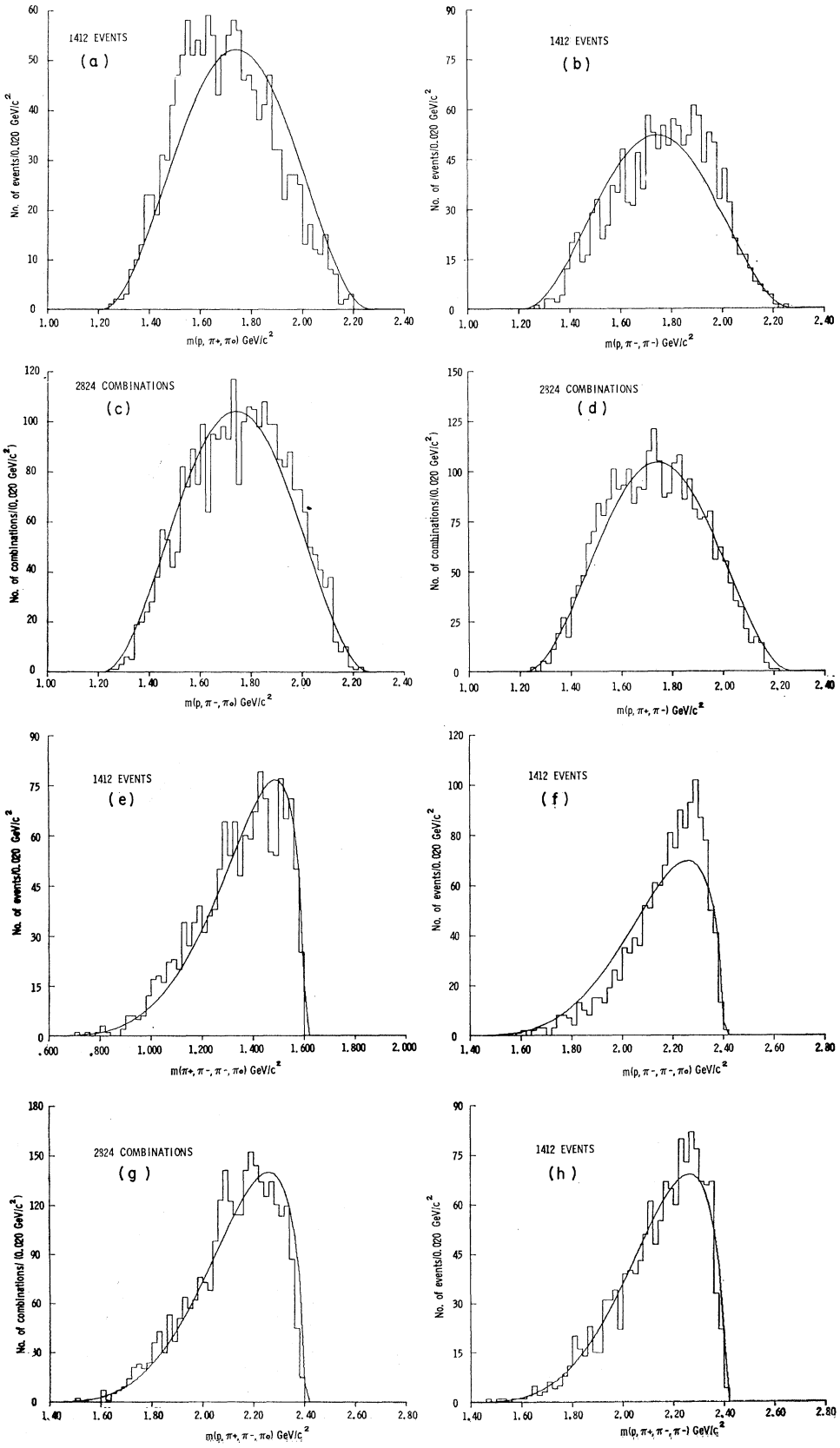

FIG. 21. Mass plots for $\pi^- p \to p\pi^+\pi^-\pi^-\pi^0$: (a) $p\pi^+\pi^0$, (b) $p\pi^-\pi^-$, (c) $p\pi^-\pi^0$, (d) $p\pi^+\pi^-$, (e) $\pi^+\pi^-\pi^-\pi^0$, (f) $p\pi^-\pi^-\pi^0$, (g) $p\pi^+\pi^-\pi^0$ (h) $p\pi^+\pi^-\pi^-$.

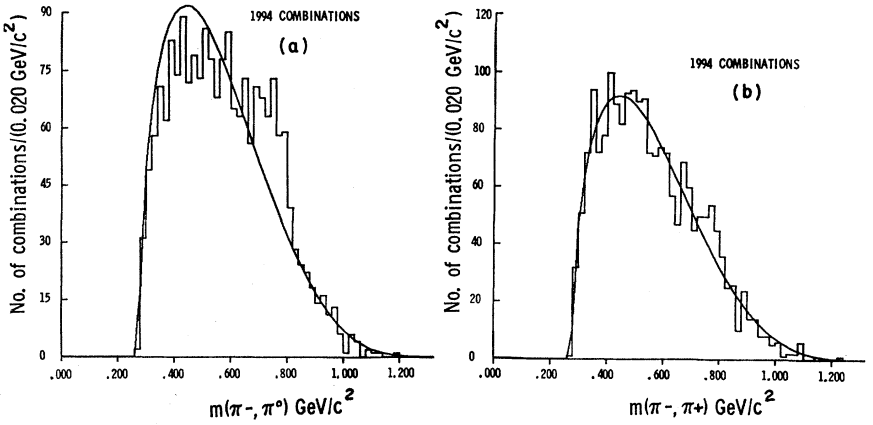

FIG. 22. (a) $m(\pi^-\pi^0)$ with ω^0 events [i.e., $0.764<m(\pi^+\pi^-\pi^0)<0.804$ GeV/c^2] excluded; (b) $m(\pi^-\pi^+)$ with ω^0 events excluded.

directly to 3π.) Subtracting the estimated number of A_2 mesons from the total, and assuming that the resultant is the number of events arising from "true" $\rho\pi$ production (as distinct from directly produced 3π events in which one $\pi^+\pi^-$ combination happens to lie in the ρ band), a value of $X\simeq 0.30\pm 0.25$ is obtained.

(iii) The statistical errors of method (ii) are reduced by considering the $m^2(\pi^+\pi^-)$ spectra for all events [Fig. 16(b)] and for events outside the A_1 and A_2 region, [Fig. 16(c)], although the uncertainty caused by ignorance of the true form of phase space remains. Assuming that the ratio of 3π to total background in these regions [estimated using arguments similar to those presented in (ii)] is identical to that for the A_2 region of the $\rho\pi$ spectrum, values of X of 0.39 ± 0.12 and 0.49 ± 0.10 respectively, are obtained.

Thus, reasonable limits on the value of

$$X\equiv\frac{3\pi \text{ background in } A_2 \text{ region}}{3\pi+\rho\pi \text{ background in } A_2 \text{ region}}$$

are taken as 0.3 and 0.6.

The form of the 3π and $\rho\pi$ backgrounds assumed are shown in Fig. 17. (These curves are arbitrarily normalized to the same number of events.) The falloff at the upper and lower values of $m^2(\pi^+\pi^-)$ arise from the kinematic limits. The contributions from each Dalitz plot throughout the region $1.24<m(\pi^+\pi^-\pi^-)<1.39$ GeV has been added together, weighted according to phase space. For the 3π case, it has been assumed that the density of points is uniform throughout each of the Dalitz plots. For the $\rho\pi$ component, it is assumed that the points contribute uniformly to the two ρ bands and that they add up in an incoherent manner in the overlap region.

The Frazer curves have been calculated using the values for the ρ and A_2 cuts given above; the full width of the experimental resolution function at half-height for $m(\pi^+\pi^-)$ is 9 MeV. Each of these distributions is then added to the background distributions for different values of X and B, and the resulting distribution is compared to the experimental one. The results are summarized in Fig. 18, where the χ^2 percentage probability value[27] is plotted as a function of B, for values of X of 0.3, 0.45, and 0.6 [Figs. 18(a)–(c)]. The χ^2 probability as a function of X for the best estimate of $B=65\%$ is shown in Fig. 18(d). The region of the plots above the horizontal dashed line is excluded at the 95% confidence level for six degrees of freedom, and the vertical dashed lines indicate the limits of X and B discussed earlier. Figure 18(e) shows the fit to the experimental projection of the Dalitz plot of Fig. 15 for the best estimates of $X=0.45$ and $B=65\%$.

It is clear that the expected 2^+ assignment for the A_2 spin and parity is favored throughout the ranges of X and B considered. It is interesting to note that if the contribution of the $\rho\pi$ background is ignored (i.e., $X=1$), the separation between the 2^+ assignment and

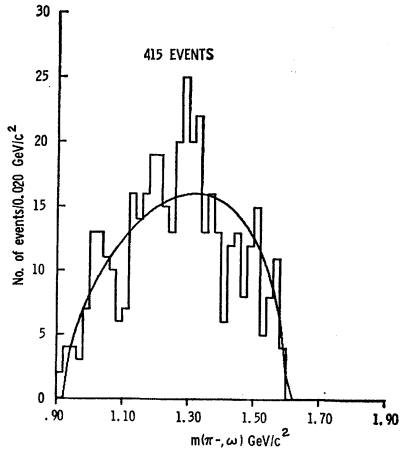

FIG. 23. $m(\pi^+\pi^-\pi^0\pi^-)$ with at least one $\pi^+\pi^-\pi^0$ combination in $0.764<m(\pi^+\pi^-\pi^0)<0.804$ GeV/c^2. The solid curve is the phase-space distribution normalized to all events.

[27] $$\chi^2=\sum_{i=i}^{N}(N_i^{\text{th}}-N_i^{\text{obs}})^2/N_i^{\text{th}},$$
where N_i^{th}, N_i^{obs}, are the theoretical and observed numbers of events in the ith bin of the histogram, and N is the total number of bins.

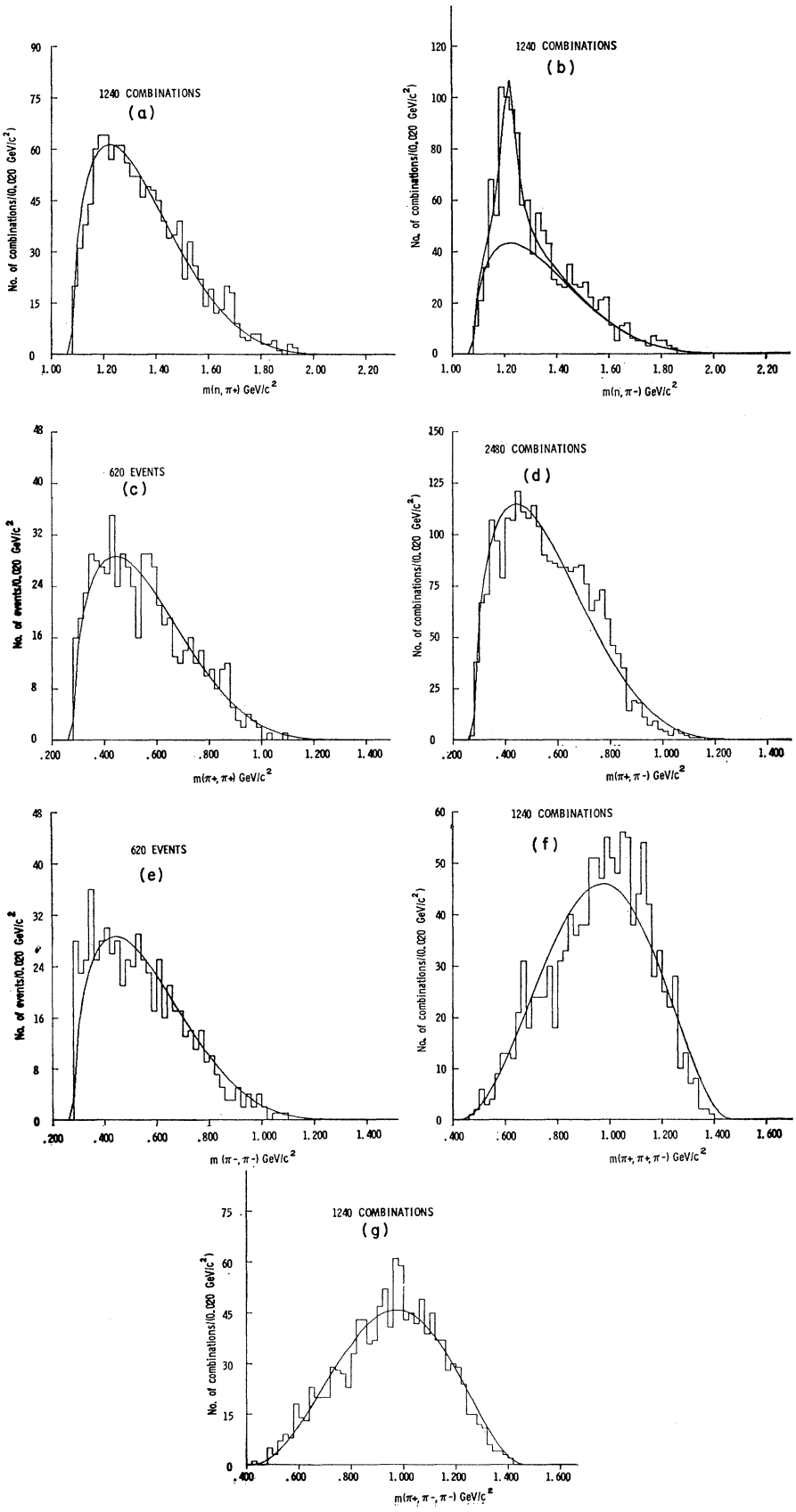

FIG. 24. Mass plots for $\pi^- p \to n\pi^+\pi^+\pi^-\pi^-$: (a) $n\pi^+$, (b) $n\pi^-$, (c) $\pi^+\pi^+$, (d) $\pi^+\pi^-$, (e) $\pi^-\pi^-$, (f) $\pi^+\pi^+\pi^-$, (g) $\pi^+\pi^-\pi^-$.

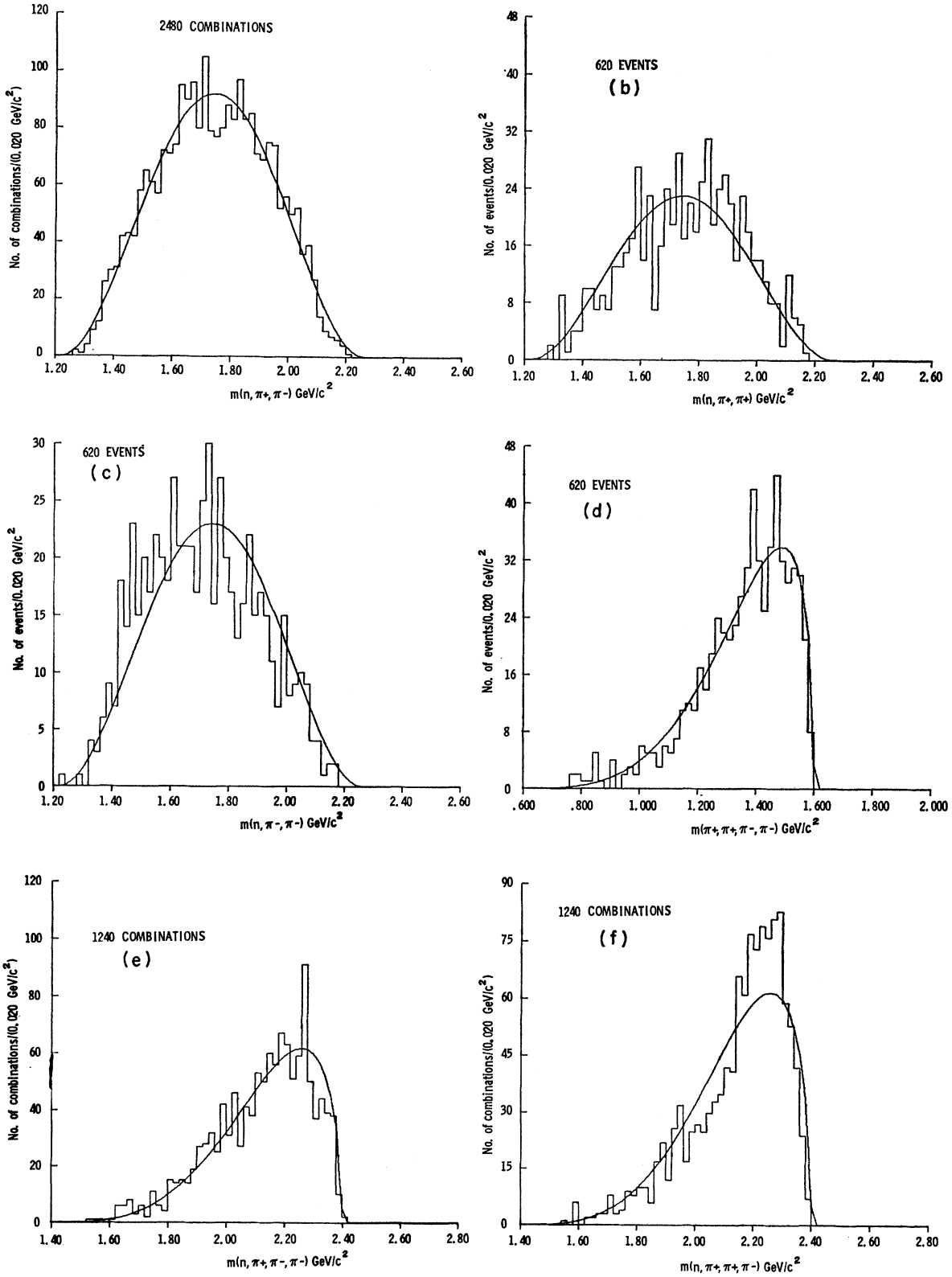

FIG. 25. Mass plots for $\pi^- p \to n\pi^+\pi^+\pi^-\pi^-$: (a) $n\pi^+\pi^-$, (b) $n\pi^+\pi^+$, (c) $n\pi^-\pi^-$, (d) $\pi^+\pi^+\pi^-\pi^-$, (e) $n\pi^+\pi^-\pi^-$, (f) $n\pi^+\pi^+\pi^-$.

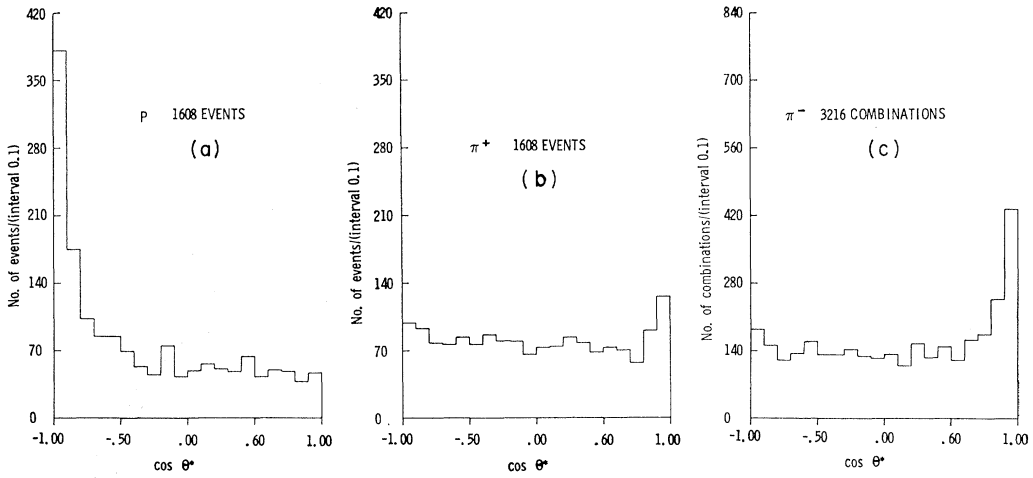

FIG. 26. Center-of-mass production angular distributions for $\pi^- p \to n\pi^+\pi^+\pi^-\pi^-$: (a) neutron, (b) π^+, (c) π^-.

the nearest competitors $[1^+(l=0)$ and $1^-]$ becomes much greater.

III. $p\pi^+\pi^-\pi^-\pi^0$ CHANNEL

(a) This channel is dominated by the production of ω^0 and $N^{*++}(1238)$. The production of ρ^-, ρ^0, and $N^{*+}(1238)$ is also observed. However, none of these resonances shows as strong a degree of peripherality as is observed in the $p\pi^+\pi^-\pi^-$ channel. This fact is reflected in the c.m. production angular distributions, Fig. 19, of the outgoing particles. Comparison of these with the corresponding distributions for the $p\pi^+\pi^-\pi^-$ channel, Fig. 2, illustrates this point. There is some evidence for the quasi-two-body $N^{*0}\omega^0$ production as was found by other workers.[2,3,28] The study of the decay angular correlations was not, however, attempted for this process as large background contamination makes the interpretation of such an analysis difficult.

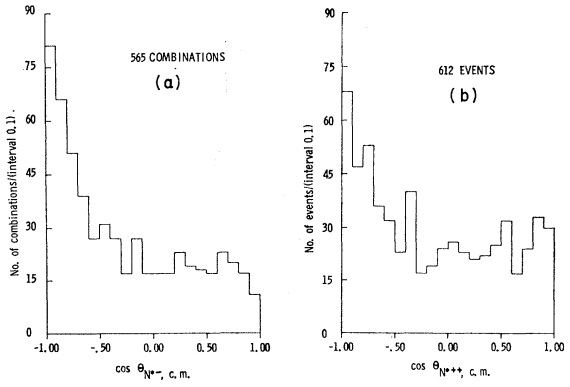

FIG. 27. (a) Center-of-mass production angular distribution for N^{*-} events in $\pi^- p \to n\pi^+\pi^+\pi^-\pi^-$ [events with $1.14 < m(n\pi^-) < 1.27$ GeV/c^2]; (b) c.m. production angular distribution for N^{*++} events in $\pi^- p \to p\pi^+\pi^+\pi^-\pi^-\pi^0$ with equivalent mass cut.

[28] J. Alitti, J. P. Baton, W. Fickinger, M. Neveu-René, A. Romano, and R. Gessaroli, Phys. Letters **21**, 354 (1966).

Figures 20 and 21 give the effective-mass distributions for all possible combinations in this channel. A BW fit to the $m(p\pi^+)$ distribution and a Gaussian fit to the $\pi^+\pi^-\pi^0$ distribution gave the following results:

Combinations $\pi^+\pi^-\pi^0$

Percentage of ω^0	$(26.0\pm2.2)\%$,
Mass	784.8 ± 1.1 MeV/c^2,
Effective full width at half-maximum	32.5 ± 2.4 MeV/c^2,
Percentage of η^0	$(3.3\pm0.8)\%$.

Combination $p\pi^+$

Percentage of N^{*++}	$(30\ \pm6)\%$,
Mass	$1204\ \pm6$ MeV/c^2,
Width	$118\ \pm22$ MeV/c^2.

Study of the Δ^2 distributions for ω^0 and N^{*++} events showed that these are much less peripheral than the corresponding distributions for ρ^0 and N^{*++} events in the $p\pi^+\pi^-\pi^-$ channel. ρ production in this channel is obscured by the reflection of the strong ω^0 production. When ω^0 events are excluded, a prominent ρ^- peak and a somewhat weaker bump for ρ^0 are revealed (Fig. 22). There is very little evidence for ρ^+ production. The enhancement at $\simeq$400 MeV in the $m(\pi^+\pi^0)$ spectrum can be expanded by ω^0 reflection.

(b) Figure 23 shows the $m(\omega^0\pi^-)$ distribution. There is no evidence for B enhancement near 1220 MeV/c^2. The $\pi^-\eta^0$ enhancement near the A_2 region was discussed in Sec. IIIB.

(c) In Fig. 21(g), two peaks appear at about 2080 and 1290 MeV. These have been discussed in more detail elsewhere.[29] They are not associated with the ω^0 production, being unchanged when the ω^0 is anti-selected. They are strongly associated with $N^{*++}(1238)$

[29] T. S. Yoon, P. Berenyi, A. W. Key, J. D. Prentice, N. R. Steenberg, and W. D. Walker, Phys. Letters **24**, 307 (1967).

events and are not reduced when the further requirement of $m(\pi^-\pi^0)$ being in the ρ^- band is imposed. They could therefore be due to the decay $N^{*+} \to N^{*++}(1238)\rho^-$. The upper one is consistent in mass, but probably not in width, with the known $N^*(2190)$ which has been assigned $J^P = \frac{7}{2}^-$.[30] Apparent corroboration for the lower, 2080-MeV, peak and its $N^{*++}\rho^-$ decay mode has appeared very recently in a study of pp interactions.[31]

IV. $n\pi^+\pi^+\pi^-\pi^-$ CHANNEL

The effective-mass distributions for all possible combinations in the neutron channel are given in Figs. 24 and 25. Strong $N^{*-}(1238)$ production is the dominant feature of this channel. A BW fit to $m(n\pi^-)$ yielded the following results:

Mass of N^{*-}	1217 ± 5 MeV/c^2,
Width	73 ± 14 MeV/c^2,
Percentage production	$(59\pm10)\%$.

There is some evidence for ρ^0 production, although it is obscured by the high multiplicity (four) of this combination.

The production of $N^{*-}(1238)$ cannot proceed by the exchange of a singly charged meson. The large cross section for this process suggests that the dominant production mechanism for the entire $n\pi^+\pi^+\pi^-\pi^-$ channel is not one-meson exchange. Production angular distributions for n, π^+, and π^- (Fig. 26) support this suggestion: No evidence for a strong peripheral reaction is observed, as was the case in the $p\pi^+\pi^-\pi^-\pi^0$ channel. The production angular distribution of N^{*-} is very similar to that of N^{*++} in the $p\pi^+\pi^-\pi^0$ channel (Fig. 27). The cross section for N^{*-} production (410 μb) is also of the same order of magnitude as that for the N^{*++} in the π^0 channel (470 μb). This suggests that both may be produced by a similar mechanism such as, for example, final-state interactions.

The fact that the N^{*-} production cross section increases with decreasing c.m. energy (see Table IV) is not inconsistent with this interpretation.

TABLE IV. Production of N^{*-} at several π momenta.

Incident π momentum (GeV/c)	$(N^{*-}\pi^+\pi^+\pi^-)/(n\pi^+\pi^+\pi^-\pi^-)\times100$	$\sigma(N^{*-})$ (μb)
2.7[a]	72 ± 12	480 ± 80
2.96	59 ± 10	410 ± 100
3.2[b]	34[c]	300 ± 50
4.2[b]	30[c]	340 ± 50

[a] See Ref. 3.
[b] See Ref. 2.
[c] The N^{*-} cross sections quoted here are double those given by Chung (Ref. 2). The mass distributions given by Chung and his estimates of N^{*-} cross sections appear to contradict by a factor of 2.

ACKNOWLEDGMENTS

It is a pleasure to thank S. Maggs and her team of scanners and measurers at Toronto and the scanning and measuring team at Argonne for the diligent and efficient work which both groups produced. The assistance of the MURA-ANL 7⁰ beam group and the crew of the 30-in. MURA-ANL hydrogen chamber is gratefully acknowledged.

[30] A. Yokosawa, S. Suwa, R. E. Hill, R. J. Esterling, and N. E. Booth, Phys. Rev. Letters **16**, 714 (1966).
[31] R. R. Kinsey, W. Chinowsky, P. Condon, S. Klein, M. Mandelkern, P. Schmidt, J. Schultz, F. Martin, M. L. Perl, and T. H. Tan, Bull. Am. Phys. Soc. **12**, 916 (1967).